

A review of chemical and physical characterisation of atmospheric metallic nanoparticles

Sanderson, Paul; Delgado Saborit, Juana Maria; Harrison, Roy M.

DOI:

[10.1016/j.atmosenv.2014.05.023](https://doi.org/10.1016/j.atmosenv.2014.05.023)

License:

Creative Commons: Attribution (CC BY)

Document Version

Publisher's PDF, also known as Version of record

Citation for published version (Harvard):

Sanderson, P, Delgado Saborit, JM & Harrison, RM 2014, 'A review of chemical and physical characterisation of atmospheric metallic nanoparticles', *Atmospheric Environment*, vol. 94, pp. 353-365.
<https://doi.org/10.1016/j.atmosenv.2014.05.023>

[Link to publication on Research at Birmingham portal](#)

Publisher Rights Statement:

Eligibility for repository : checked 09/06/2014

General rights

Unless a licence is specified above, all rights (including copyright and moral rights) in this document are retained by the authors and/or the copyright holders. The express permission of the copyright holder must be obtained for any use of this material other than for purposes permitted by law.

- Users may freely distribute the URL that is used to identify this publication.
- Users may download and/or print one copy of the publication from the University of Birmingham research portal for the purpose of private study or non-commercial research.
- User may use extracts from the document in line with the concept of 'fair dealing' under the Copyright, Designs and Patents Act 1988 (?)
- Users may not further distribute the material nor use it for the purposes of commercial gain.

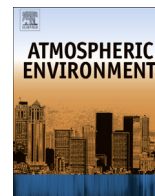
Where a licence is displayed above, please note the terms and conditions of the licence govern your use of this document.

When citing, please reference the published version.

Take down policy

While the University of Birmingham exercises care and attention in making items available there are rare occasions when an item has been uploaded in error or has been deemed to be commercially or otherwise sensitive.

If you believe that this is the case for this document, please contact UBIRA@lists.bham.ac.uk providing details and we will remove access to the work immediately and investigate.



Review

A review of chemical and physical characterisation of atmospheric metallic nanoparticles



Paul Sanderson, Juana Maria Delgado-Saborit, Roy M. Harrison*

Division of Environmental Health & Risk Management, School of Geography, Earth & Environmental Sciences, University of Birmingham, Edgbaston, Birmingham B15 2TT, United Kingdom

HIGHLIGHTS

- Nanoparticles are an intense topic of research and have important health implications.
- On-line and off-line sampling methods are considered.
- Measured airborne concentrations of specific metals are reviewed.
- Small number of receptor modelling studies published to date.
- Sources and tracers of nanoparticle sources are reviewed.

ARTICLE INFO

Article history:

Received 20 December 2013

Received in revised form

7 May 2014

Accepted 9 May 2014

Available online 10 May 2014

Keywords:

Particulate matter

Nanoparticles

Ultrafine particles

Metals

ABSTRACT

Knowledge of the human health impacts associated with airborne nanoparticle exposure has led to considerable research activity aimed at better characterising these particles and understanding which particle properties are most important in the context of effects on health. Knowledge of the sources, chemical composition, physical structure and ambient concentrations of nanoparticles has improved significantly as a result. Given the known toxicity of many metals and the contribution of nanoparticles to their oxidative potential, the metallic content of the nanoparticulate burden is likely to be an important factor to consider when attempting to assess the impact of nanoparticle exposure on health. This review therefore seeks to draw together the existing knowledge of metallic nanoparticles in the atmosphere and discuss future research priorities in the field. The article opens by outlining the reasons behind the current research interest in the field, and moves on to discuss sources of nanoparticles to the atmosphere. The next section reviews ambient concentrations, covering spatial and temporal variation, mass and number size distributions, air sampling and measurement techniques. Further sections discuss the chemical and physical composition of particles. The review concludes by summing up the current state of research in the area and considering where future research should be focused.

© 2014 The Authors. Published by Elsevier Ltd. This is an open access article under the CC BY license (<http://creativecommons.org/licenses/by/3.0/>).

1. Introduction

The term nanoparticle (NP) is used to refer to a wide range of particles, and definitions vary considerably between different studies, depending on the context of the study and the technique of measurement. It is most frequently used as a specific size description (usually < 100 nm, though sometimes < 50 nm) and this review will use the term nanoparticle to refer to particles of

<100 nm, interchangeably with the term ultrafine particle (UFP, taken to mean $PM_{0.1}$). If the study being referred to used these term differently this will be stated. Likewise, the terms atmospheric, airborne and ambient will be used interchangeably, and refer to outdoor and indoor non-occupational environments. Many sources also refer to particle modes – nuclei, Aitken, accumulation, coarse – and definitions of these modes also vary greatly. This subject is discussed at length in a review of atmospheric nanoparticles (Kumar et al., 2010). Some recent studies of UFP have included larger particles up to 180 or even 250 nm aerodynamic diameter (Daher et al., 2013; Ntziachristos et al., 2007; Saffari et al., 2013). The cut-off point between ultrafine and accumulation modes is not clear; a large fraction of accumulation mode particles are sourced from UFP, and due to the fractal structures of soot particles,

* Corresponding author. Also at: Department of Environmental Sciences/Center of Excellence in Environmental Studies, King Abdulaziz University, PO Box 80203, Jeddah 21589, Saudi Arabia.

E-mail address: r.m.harrison@bham.ac.uk (R.M. Harrison).

particles with measured diameter >100 nm may be comprised of small sub-particles within the nanoparticle size range.

Much of the concern over atmospheric nanoparticles derives from their possible effects on human health. These are outside of the scope of this article and the reader is referred to a recent review on the subject (Heal et al., 2012).

2. Origin and sources of metallic nanoparticles

There are a wide range of known sources of metallic particles in the ultrafine size range, contributing many different elements to the particulate mass in a number of different chemical or physical forms. Among the more commonly observed metals in ultrafine aerosol are Na, Ca, K, Al, Fe, Pb, Ni, Cr, Ti, V and Zn, but a number of less abundant elements such as U and Ce have also been observed (Bzdek et al., 2012). Some common associations with known sources appear in Table 1.

In recent years there has been growing appreciation of the significance of metallic nanoparticles in the atmosphere. In particular, the nanoparticle fraction of metals produced by road traffic appears to be increasing as a proportion of the total particulate matter emitted by motor vehicles, owing to the increasing use of metallic fuel additives, catalysts and diesel particulate filters (Liati et al., 2012) and additives in lubricating oil (Miller et al., 2007b). Particularly important are metallic fuel borne catalysts (Jung et al., 2005; Park et al., 2008a; Nash et al., 2013; Gidney et al., 2010; Lahaye et al., 1996), the aim of which is to reduce the total inhalable particulate matter fraction. In doing so they fundamentally change the morphology and distribution of emitted particles, decreasing the size of soot particles (Morawska et al., 2009).

It has been reported that 50% of metal-containing nanoparticles contain more than one metal (Adachi and Buseck, 2010). Fe, Zn, Ni, Cr and Ti are often found in particles containing two or more metals. Particular combinations of multiple elements have sometimes been found to be specific to particular sources or processes, enabling these particle classes to be used as markers (Bzdek et al., 2012) or to demonstrate common emission sources. For instance, Tolocka et al. (2004) in a study in Baltimore discovered that Fe particles were detected under certain wind conditions, and 62% of these particles also contained Pb. They were able to assign these particles to emissions from a medical waste incinerator near to the sampling site (Tolocka et al., 2004).

Table 1
Metals in ultrafine particles associated with known sources.

Source type	Associated elements	Reference
Diesel	Al, Ca, Cu, Fe, Mg, Mn, V, Zn	Liati et al., 2012; Patel et al., 2012
Gasoline (emissions)	Sr, Cu, Mn	Lin et al., 2005
Lubricating oil	Fe, Ca, P, Zn, Mg	Gidney et al., 2010
Fuel-borne catalysts	Fe, Mn, Ce	Park et al., 2008a; Cassee et al., 2011
Diesel fuel (marine engines)	Al, Ca, Fe, Ni, V, Zn	Lyyräinen et al., 1999; Moldanová et al., 2009; Kumar et al., 2012
<i>Non-exhaust traffic sources</i>		
Brakes	Fe, Cu, Sn, Zn	Kukutschová et al., 2011
Tyres	Cd, Co, Cr, Cu, Fe, Mn, Pb	Adachi and Tainosho, 2004
Road dust	Zn, Al, K, Fe, Na, Mn	Saffari et al., 2013; Daher et al., 2013
<i>Industrial sources</i>		
Metalworking	Fe, K, Na, Pb, Zn	Reinard et al., 2007
Power generation	Ce, Fe, La, Na, K, V,	Reinard et al., 2007; Linak et al., 2007;
Incinerators	Cd, Pb, Sb, Zn	Tolocka et al., 2005

2.1. Crustal origin

Studies of the Si/Al relationship in ambient aerosols have revealed an extremely close correlation between the concentrations of the two elements, thereby demonstrating that the main source is likely to be crustal (Kenneth, 1976). This study also suggests, however, that fly ash and anthropogenic dust may affect the Si/Al ratios in urban areas. However, while the diagnostic use of the ratio is considered to be useful for PM_{2.5} or PM₁₀, it is less likely to be valid for the ultrafine size fraction, due to the presence of Al in diesel exhaust particles (Bérubé et al., 1999). Since such particles are prime contributors to urban ultrafine aerosol, this will skew the Si/Al ratio compared to crustal reference materials. Furthermore, Lin et al. (2005) reported that Al, Si, Ca and Fe all exhibited ultrafine Aitken modes (below 100 nm), which implies that local combustion sources are responsible for most particles of these elements in this size range (Lin et al., 2005). This has clear – but so far little discussed – implications for the validity of using these elements as crustal tracers in the ultrafine size range.

Many studies have used concentrations normalised to aluminium for other metal concentrations in order to calculate enrichment factors (Ntziachristos et al., 2007; Dodd et al., 1991). Ntziachristos et al. (2007) reported that although it was not possible to rule out an anthropogenic contribution to roadside Al, Al abundance did not exceed its upper continental crust enrichment level in any of the samples they collected. Park et al. (2008b) have also found that Ca concentrations in ultrafine particles collected in Gwangju were significantly enriched during an Asian dust event, although the total UFP mass did not increase (Park et al., 2008b).

2.2. Industrial processes

Waste incinerators are known to be a source of trace metals in atmospheric particulates, although abatement technology on modern incinerators is designed to limit their emissions to low levels (Buonanno et al., 2009; Nixon et al., 2013). ZnCl₂ is a prominent component, while Sb, Cd and Pb are also known to be emitted by incinerators. These three metals in combination have been used as a marker for incinerator emissions (Tolocka et al., 2005). A previous study reported that number size distributions of particles containing V, Fe, As and Pb peaked at 150 nm in Baltimore (Tolocka et al., 2004), indicative of combustion and incineration sources. Some studies consider this size range relevant to the ultrafine. Cernuschi et al. (2012) reported that metals accounted for 17% of total PM mass below 50 nm and 22% below 100 nm emitted from four waste to energy plants, and observed that particle formation mechanisms are similar to solid fuels such as coal. The main metals in ultrafine and nanoparticle emissions (100 nm and 50 nm respectively) were Cr, Fe, Ni, Pb and Zn. Traces of Ti, V, Mn and Co were also detected (Cernuschi et al., 2012). Buonanno et al. (2011) measured metal content in particles of 50, 100, 150 and 200 nm. Concentrations of metals with boiling points below 1200°C (As, Cd, Zn) were found to decrease with increasing particle size and metals with higher boiling points (Co, Cr, Fe, Sb, Sc, Sm, Th, Eu, Yb) to increase with particle size, as the more volatile elements boiled and then nucleated during cooling. The less volatile elements remained in the solid phase (Buonanno et al., 2011). However, modern energy from waste plants have extremely low nanoparticle emissions (Buonanno et al., 2009; Ragazzi et al., 2013).

Many metals are also emitted by coal combustion, such as in power generation. Linak et al. (2007) reported that fly ash particles below 500 nm contained elevated concentrations of more volatile metals such as Na, K and V. Fe is the most important metal and is reported to occur quite uniformly in all size fractions, with

nanoparticulate γ -Fe₂O₃ being especially prominent below 500 nm (Linak et al., 2007).

Zn and Ni concentrations measured in ultrafine particulate matter by Park et al. (2008b) in Gwangju, Korea, were found to exhibit a strong wind direction dependence which tied them to a nearby industrial complex, from which the main sources were metallurgical processes (Park et al., 2008b).

2.3. Traffic: exhaust and non-exhaust sources

Emissions from road vehicles are the primary source of metallic nanoparticles to the atmosphere. These can include combustion derived material from internal combustion engines, the metallic content being derived from lubricating oils, fuel additives and trace amounts in gasoline and diesel fuels, particles from brake wear (Gietl et al., 2010), and from resuspended tyre dust.

2.3.1. Exhaust sources

Miller et al. (2007b) attempted to isolate the effects of lubricating oil additives by using TEM-X-EDS to analyse particles generated in a hydrogen-fuelled engine. It was found that soot agglomerates were rare, while four types of metal-bearing particle were common. High density metallic spheres formed of Fe, Ca, P, Zn and Mg were seen across a wide size range (30–300 nm; such particles tend to be at the smaller end of this range in diesel and become associated with soot) and probably originate from self-nucleation of dense elements like Fe and Ca coated with more volatile components, which condense onto the surface during cooling. Less dense spheres, containing less Ca, were also seen. In some cases the volatile components formed shells around metals. Spherical nanoparticles, mainly composed of Fe, were observed and likely formed immediately after combustion by self-nucleation. Some carbonaceous particles were attributed to homogenous nucleation of hydrocarbon vapours (Miller et al., 2007b). Al and V are both associated with combustion processes. Al is most likely to derive from wear to mechanical parts in the engine itself, while V is naturally present in oil and is often used as a marker for fuel oil burning (Tolocka et al., 2004).

Diesel exhaust is the most important traffic-related nanoparticle source. A study in Mexico City (Adachi and Buseck, 2010) discovered that around 70% of metal nanoparticles were embedded in or attached to particles containing soot with 13% in particles of organic and sulphate compounds, but only around 1% were in soot particles not associated with organics and sulphate. The authors proposed that condensation involving organics and sulphate led to this association in polluted air. However, a lack of obvious correlation between metallic nanoparticle composition and soot concentration implies that many metallic NPs are incorporated during atmospheric transport. Diesel soot, being formed by high temperature combustion or pyrolysis of hydrocarbons, consists primarily of carbon, with small amounts of oxygen and hydrogen. However, other elements can become associated with it through interactions with lubricating oils. Among these components are P, S, Ca and Zn (Patel et al., 2012). Liati et al. (2012) investigated the inorganic ash components of diesel emissions deposited in the diesel particulate filter of a light truck using TEM-X-EDS. They found the inorganic particles to be highly variable in size (7–12 to 170 nm) and to consist mainly of Ca, Mg, P, Zn, S and O with some Al and Fe. Some of this material reached the ambient air, some but not all associated with soot. These findings were similar in a passenger car using Fe-doped fuel, but in this case the typical particle size was smaller; from 4 to 40 nm (Liati et al., 2012).

Fewer data are available concerning gasoline engine exhaust; however, Lin et al. (2005) reported that relative abundances

(normalised to upper continental crust) of several metals (Sr, Cu and Mn) in ambient samples in the 56–100 nm size range were similar to those in gasoline exhaust, and strikingly different to those in diesel soot. By contrast, Ba, Pb and Zn showed similar relative abundance in the 56–100 nm range to diesel soot (Lin et al., 2005). It has been reported that metallic additives (Mn, Fe, Pb) cause significant changes to particle size distributions from gasoline engines. While untreated fuel exhibited a unimodal distribution with only an accumulation mode which was attributed to hydrocarbon removal by the three-way catalyst, metallic species increased number concentrations in the ultrafine mode. Treatment with a catalytic stripper demonstrated that the nucleation mode particles were largely composed of inorganic material. Furthermore, Fe and Mn, which are able to condense at around 1250 °C, were present in much higher amounts than Pb, which remains in the gas phase down to 650 °C (Gidney et al., 2010). Kittelson et al. (2006) carried out a detailed investigation of on-road number distributions from spark-ignition gasoline engines and determined that emissions were low under cruise conditions but under heavy acceleration, distributions similar to diesel engines were produced. Source apportionment showed that number concentration was dominated by heavy duty diesels, except at weekends when light duty gasoline engines became more important (Kittelson et al., 2006).

2.3.2. Fuel additives

The increasing use of fuel-borne oxidation catalysts to improve engine performance is currently a cause for concern as these can add species and quantities of potentially harmful metals to the ultrafine particulate burden which would not otherwise be present.

Recent studies (Park et al., 2008a; Cassee et al., 2011) have shown that nanoparticulate CeO₂ is present in ambient air, resulting from use as an additive in diesel fuels. Ceria is generally added to diesel as nanoparticles resuspended in an organic matrix to make them miscible with diesel fuel. For example, the nanoparticulate ceria additive Envirox is suspended in a hydrocarbon carrier at 2% w/v, and diluted with diesel at 1:4000 for a concentration of 5 mg dm⁻³ in fuel. This approach is considered superior to coating particulate filters in the catalyst, which suffers from catalytic poisoning by combustion gases (Lahaye et al., 1996). Functioning as an oxygen donating catalyst, it can improve and extend fuel burn and enhances the performance of particulate filters by oxidising deposited material, such as hard carbon deposits. While particulate emissions as a whole are found to decrease if CeO₂ is used (by approximately 15%), according to Park et al. (2008a). Emissions in the nanoparticle range are found to increase (Park et al., 2008a). Jung et al. (2005) tested the impact of adding Ce to a medium duty diesel engine, discovering that the number of accumulation mode particles decreased while the number of nucleation mode particles increased; they attributed this to the reduction in the available surface area reducing the scavenging of particle precursors, thereby leading to more homogenous nucleation and reduced coagulation of nucleation mode particles with particles in the accumulation mode (Jung et al., 2005).

Metallic additives using other metals are also available. Optimax 4804, tested in diesel at 200 ppm by Song et al. (2006), contains a 4:1 ratio of Fe:Sr. Especially at light loads, this additive yielded a significant reduction in total soot especially at lower engines loads, but led to metal oxides being detected in the soot aggregates (Song et al., 2006). Ferrocene has also been tested as a fuel borne catalyst (Lee et al., 2006), introduced into the fuel by dissolving ferrocene powder in a small volume of diesel then blending with the bulk fuel to the desired concentration. Ferrocene doping was found to produce Fe-rich nanoparticles, whose size and concentration increase with doping level.

Lenin et al. (2013) recently tested additives prepared from MnO and CuO, MnO being found to be the more effective of the two. As in the ferrocene and ceria studies, soot production was found to be reduced but to include metal oxides from the catalyst in inhalable particles (Lenin et al., 2013).

2.3.3. Non-exhaust traffic sources

Material derived from brake wear can originate either from abrasive processes (which tend to produce particles in the fine and coarse modes) or from volatilisation of metals due to heating, which tends to produce ultrafine particles. Ba, Sb, Mg, Cu, Fe and Zn are all present in brake materials and therefore associated with PM derived from this source (Gietl et al., 2010). Metal silicates and mineral fibres have also been associated with brake linings (Hays et al., 2011). Composition of brake discs and linings varies considerably between manufacturers and applications, however, so wide ranges of composition are possible in emitted particles from this source. At sites where traffic emission predominates, brake wear appears to be the main source of these elements. Ba, which is unlikely to have many other sources, can be used as a tracer for brake wear in fine PM (Gietl et al., 2010). Evidence from roadside studies suggests this is also possible for ultrafine PM. For example, Ntziachristos et al. (2007) found that Sb, Fe, Ba and Cu, all associated with brake wear by earlier studies, showed significantly higher concentrations at a roadside site both in PM_{0.18} and PM_{2.5}, illustrating both abrasive and volatilising processes contributing these elements, with the enrichment being more significant in the accumulation mode than the ultrafine mode. Evidence of nanoscale wear particles being produced has been found in laboratory tests. Garg et al. (2000) found that between 26 and 44% of the total mass of emitted brake particles were 100 nm or less (Garg et al., 2000). Kukutschová et al. (2011) reported that the nanoscale particles differed considerably in chemical composition from larger wear particles and from the bulk composition of the brake material, owing to the high temperatures and pressures at the friction interface. Cu, Fe, Sn and Zn were confirmed in nanoscale particles, but although Mo, Al and Pb were found in the bulk material they were not confirmed in the smallest wear particles (Kukutschová et al., 2011). These elements have been detected in ambient PM_{0.25}, associated with the road dust fraction at urban sites and separate from it at rural ones, probably due to the dominance of traffic sources making apportionment at urban sites more difficult (Saffari et al., 2013).

Tyre dust contributes metallic particles to aerosol from a number of sources (Adachi and Tainosho, 2004). ZnO is particularly important but other metals including Mn, Fe, Co, Ni, Cu, Cd and Pb are also emitted. While tyre wear is often associated with coarse particles, Dahl et al. (2006) present evidence showing that nanoparticles are also emitted. Mean particle number diameters were found to be between 15 and 50 nm, with emission factors increasing with speed. Compared to an emission study assuming a light-duty vehicle fleet of 95% gasoline and 5% diesel vehicles, the emission factors corresponded to 0.1–1% of tailpipe emissions (Dahl et al., 2006). Gustafsson et al. (2008) also reported nanoparticle generation from tyre-surface interfaces (Gustafsson et al., 2008).

Tyre dust is known to include particles which are not originated from the tread, but from brake dust, paint and abraded asphalt, each of which has distinct chemical and morphological characteristics (Adachi and Tainosho, 2004). Aggregate oval particles of PbCrO₄ are particularly associated with abraded particles of yellow paint, high levels of iron and Cu/Sb ratios of 4.6 ± 2.3 with brake wear particles and multi-angular ZnO containing particles with tyre tread, although the ZnO content of tread can vary significantly. So far, the determination of tracer elements and/or diagnostic ratios

for tyre dust have proven unsuccessful. Zn has several other sources and there are no other metals associated only with tyre wear in the way Ba appears to be for brake material (Thorpe and Harrison, 2008). These authors suggest that while it may be possible to assign tracer elements through experimental measurements, the results would only be specific to that site (Thorpe and Harrison, 2008). Elements associated with road dust resuspension such as Al, K, Fe, Na and Mn have been reported in ambient samples below 250 nm by Saffari et al. (2013) and Daher et al. (2013). Furthermore, these have been found to correlate with organic carbon concentrations, linking them to motor vehicle emissions.

2.3.4. Emissions from residual oil fuel – marine diesel engines

In or near ports, nanoparticle pollution from heavy duty marine diesels will also be relevant. The physico-chemical characteristics of emissions from engines using low-grade residual fuel oils are quite different to automobile diesel engines, owing to the higher ash and aromatic content, the high air to fuel ratio which should produce less carbon soot, and the more variable conditions inside the cylinders (Lyyräinen et al., 1999). Existing data regarding medium duty marine diesels show bimodal particle size distributions, in which the modes are found at 60–90 nm and 7000–10,000 nm. The primary particles have been determined to be spherules, formed by nucleation of ash from metallic contaminants – V and Ni are particularly prominent, but Al, Ca, Zn and Na were also observed (Lyyräinen et al., 1999). The mass distributions of these elements generally follow the bimodal structure of the PM distribution, but compared to V and Ni, Ca and Zn have larger coarse modes. Moldanová et al., (2009) found three main metal-bearing morphologies in emissions from residual oil fuels: soot aggregates of carbon containing V, Ni and S, dominating PM_{1.0}; char and char mineral particles (200–5000 nm) consisting of carbonaceous spheres, in some cases quite pure but in others high in V, Ni, Ca and Fe; mineral ash of prismatic crystals (CaO, CaSO₄, CaCO₃, NiS and V₂O₃ were all identified), which were often found embedded in carbonaceous matrices. They also found carbon based particles originating from uncombusted fuel and lubricating oils. The authors concluded that morphological and composition structures in ship-exhaust residuals are very different from typical soot-like particles associated with emissions from other sources (Moldanová et al., 2009; Kumar et al., 2012). Saffari et al. (2013) detected a class of V–La–S particles in samples collected at Long Beach, directly affected by ship emissions, but found that this class could not be resolved by Principal Component Analysis at receptor sites inland (Saffari et al., 2013).

2.4. Biomass burning and wood fuels

Evidence for metals in ultrafine particle emissions from these sources has been reported. Different fuel types and combustion conditions produce very different particle types and composition, so it is not thought possible to suggest universally applicable tracer elements, although it is possible to distinguish between softwood and hardwood particle emissions (Kleeman et al., 1999). Tissari et al. (2008) reported that combustion of birch wood produced ultrafine ash particles. Metallic content was dominated by K and Zn, with Ca, Fe, Mg and Na also observed in some particles. These particles were found to be formed under ideal combustion conditions. Under incomplete combustion, carbonaceous particles dominated (Tissari et al., 2008). Kleeman et al. (1999) reported that particle mass distributions from wood smoke from pine, oak and eucalyptus exhibited a single mode peaking between 100 and 200 nm aerodynamic diameter, determined gravimetrically from samples collected by MOUDI. Several metals were observed in these samples. K showed similar distributions in emissions from all

Table 2
Reported concentrations of trace elements in ultrafine particles (all ng/m³).

Study	Chuang et al., 2012	Lü et al., 2012	Ntziachristos et al., 2007	Hughes et al., 1998	Pakkanen et al., 2001	Cass et al., 2000	Park et al., 2008b	Saffari et al., 2013			
Instrument	MOUDI	nanoMOUDI	nanoMOUDI	MOUDI	Berner Low-pressure Impactor	MOUDI	4-stage LPI	SPCI			
Metric	PM _{0.1}	PM _{0.1}	PM _{0.18}	PM _{0.097}	PM _{0.1}	PM _{0.056-0.1}	PM _{0.132}	PM _{0.25}			
Location	Coach station, central Taipei City, Taiwan	Xujiahui, Shanghai, China (urban rooftop site)	Nr I-710 freeway, South Gate, CA	Pasadena, California winter	Urban: Vallila, Helsinki, Finland	Central Los Angeles	Rooftop urban background site, Gwangju	Long Beach	Los Angeles	Riverside	Lancaster
Season	Sept–Nov	Dec–Jan	Feb–Apr	Jan–Feb	Annual mean	Aug–Sept	Annual mean	Annual mean			
<i>Element</i>					Urban	Rural					
Ag					3.70×10^{-3}	5.90×10^{-3}		0.04	0.01	0.04	0.02
Al			~6		0.51	0.44		24.7	4.58	13.1	17.8
As	0.76 ± 0.53	2.16			0.016	0.01	0.6	0.04	0.01	0.02	0.01
Ba			~1 to 2	1.04	0.058	0.031	19				
Be							<0.01				
Bi					1.90×10^{-3}	1.70×10^{-3}					
Ca		6.23	~6		2.2	1.9	200	23.8	5.36	12.7	11.6
Cd	0.12 ± 0.03			0.061	3.50×10^{-3}	2.40×10^{-3}	0.19	0.06	0.01	0.01	0.03
Ce				0.19			1.2				0
Co	0.07 ± 0.08				0.024	0.023		0.02	0	0.01	0.02
Cr	0.52 ± 0.49	0.69		7.32			6.7	0.35	0.17	0.51	0.11
Cs				0.016			0.1				
Cu	7.24 ± 8.38	7.34	~1 to 2		0.14	0.17		1.71	1.2	1.15	0.57
Eu				0.013			0.2				
Fe	9.49 ± 12.57	14.38	35	67.5	1.8	0.73	186	150	37.8	10.9	17.5
Hg				5.20×10^{-3}			0.09				
K					0.86	1.3	88	300	14.4	4.36	9.32
La				0.11			0.021		0.02	0.01	0.01
Li					2.50×10^{-3}	1.60×10^{-3}			0.03	0.01	0.03
Lu				3.80×10^{-4}			0.014				
Mg					0.26	0.27		3	6.01	1.22	3.61
Mn	0.96 ± 0.95	0.48		0.74	0.035	0.014		~1	0.79	0.17	0.42
Mo	2.25 ± 0.24			7.20×10^{-2}	0.015	0.013	0.48		0.18	0.03	0.06
Na			~6	27	2.9	1.3	85		10.6	2.67	5.24
Ni	4.57 ± 1.33	0.61			0.24	0.24			0.27	0.11	0.23
Pb	7.89 ± 4.36	4.88						8	0.46	0.13	0.32
Rb		0.14			2.80×10^{-3}	6.60×10^{-3}			0.04	0.01	0.02
Sb					0.022	6.00×10^{-3}		4	0.25	0.12	0.12
Sc							0.028				0.07
Se	0.62 ± 0.53	0.08			0.032	0.035		0.6			
Sm				0.015			0.012				
Sn									0.24	0.74	0.09
Sr	1.41 ± 1.40	0.03			0.01	9.00×10^{-3}			0.26	0.08	0.11
Th				6.50×10^{-3}	1.90×10^{-4}	9.60×10^{-4}					0.15
Ti	1.56 ± 1.63	0.43	~1 to 2	7.65	0.04	0.034	43		3.09	0.69	1.1
Tl					2.20×10^{-4}	2.00×10^{-4}					3.26
U											
V	5.65 ± 3.65	4		0.059	0.16	0.092		0.2	0.87	0.19	0.18
Yb		2.06		2.80×10^{-3}			0.26				0.16
Zn	54.71 ± 66.61		~1 to 2	3.68	0.81	0.7	3.8	50	3.09	0.89	1.07

three fuels, while other trace metals varied more, probably due to differences in the soil composition and climate conditions the woods grew in. Pine particles were associated with Fe, Rb and Ti, oak with trace levels of Al, Ba, Fe and Zn and eucalyptus with Al, Ba, Fe, Rb, Sr and Ti (Kleeman et al., 1999).

3. Concentrations and exposures

3.1. Mass concentration of metals in ultrafine and quasi-ultrafine particles

Table 2 contains mass concentration data for metals in size fractions below 250 nm diameter. These field measurements indicate a remarkable diversity of metal concentrations in the ultrafine and pseudo-ultrafine size fractions, both in absolute terms and relative to other elements.

A recent study by Boogaard et al. (2011) in the Netherlands demonstrated that there were particularly strong contrasts in the concentrations of a number of substances indicative of traffic emissions measured at roadside and background sites. Cu, Fe, Cr and black carbon were significantly elevated at roadside sites. Similarly, particle number concentrations in the 30–100 nm range were also elevated at roadsides. (Boogaard et al., 2011).

Lough et al. (2004) also found that Zn, Ba and Sb (wear elements) exhibited size distributions similar to crustal elements due to being sourced from resuspended road dust. They reported sub-micrometre modes indicative of combustion processes and/or high temperatures for Fe, Cu, Pb and Ca, with lead and copper also possessing an ultrafine mode suggestive of a source in non-mechanical processes (brake surface vaporisation, combustion of fuel and lubricating oil). Some elements, such as Cu, Sb, Zn and Ba, associated with road dust were observed at times when more heavy duty traffic was present during weekdays, correlating with a greater mass of coarse particles from resuspension (Lough et al., 2004).

Ntziachristos et al. (2007) found that the road traffic influence in $PM_{0.18}$ became more pronounced at the higher end of this size range, as the ratio of heavy-duty to light duty vehicle emission factors increases. Such emissions contain a greater proportion of fractal soot agglomerates in the upper end of the ultrafine size range; many of these particles have large mobility diameters even though their aerodynamic diameters are relatively small, owing to their low density (Ntziachristos et al., 2007). Their measurements at a California traffic roadside with around 20% heavy-duty diesel traffic found Fe to be the most abundant metal in $PM_{0.18}$ followed by Ca, Al and Na and lower levels of Ba, Cu, Zn and Ti. They also determined that most metals fell into two concentration profiles. Some elements including V, Fe, Sn and Ba showed monotonic distributions (a uniform increase in concentration with size) and originated primarily from abrasive mechanical processes or represented crustal materials. However, Mg, Al, Ca, Cu, Zn and Pb revealed similar concentrations across the lower size range, resulting in a flatter distribution. They found that Ca, Cu and Pb had similar absolute concentrations in the size ranges 18–32 nm, 32–56 nm, 56–100 nm and 100–180 nm, even though total PM concentration and total trace element concentration rose significantly over this range. The mode 18–32 nm had elevated concentrations of a range of metals, which showed a formation pathway by condensation onto metallic particles and shows that per unit mass, this size range makes a larger contribution to heavy and transition metals.

A study using a MOUDI to collect samples at a coach station in Taipei found that the bulk of the metallic mass below 1 μm occurs in the $PM_{0.1-1}$ size range, with about one third of that mass in the

$PM_{0.1}$ range. Zinc was by far the most abundant metal in the $PM_{0.1}$ size range, followed by Fe, Cu, Pb, V and Ni (Chuang et al., 2012).

The results published by Hughes et al. (1998) form an interesting comparison to Ntziachristos et al. (2007) in that there are similar trends within this group of elements but the actual mass concentrations are in many cases around twice as high. Hughes et al. (1998) also reported that they were unable to identify 23–40% of the total ultrafine particle mass, the large range being caused by the small masses available for analysis. In central Los Angeles, Cass et al. (2000) reported much higher concentrations of Ba, Cd and Ti than Hughes along with nearly three times as much Fe. UFP were found to be of similar composition to bulk $PM_{2.5}$.

More recent measurements in the Los Angeles area have been performed by Saffari et al. (2013) using Sioutas personal cascade impactors at 10 sites. This study extends the analysis to all particles below 250 nm aerodynamic diameter (quasi-ultrafine). The most abundant elements at all sites were Al, Ca, Fe, K and Na whose mass concentrations ranges ranged from 50 ng/m^3 to 200 ng/m^3 , while trace element concentrations were in the range below 10 ng/m^3 (Saffari et al., 2013). Concentrations of elements related to shipping such as V and La were found to decrease with distance from the source, to the extent that this component was not identifiable by PCA in the data from inland receptor sites.

The near-highway study by Hays et al. (2011) differs in the selection of a road with an extremely high proportion of light-duty gasoline fuelled vehicles (95% of the total 125,000 vehicles per day). In this case, inorganic material was found to account for ~7% of total mass in $PM_{0.1}$. The dominant metals in $PM_{0.1}$ were found to be K and Ca. The next most important elements were Zn and Al followed by Ti and Fe. Ni, Cr, Pb, Sb and Cu were all observed around an order of magnitude below these elements along with Ce. Zn and Ca were found to correlate in $PM_{0.1}$ indicating a common source in lubricating oil. Fe, Ba, Cu and Sb – the brake wear elements – were seen to correlate closely throughout all three size ranges ($PM_{0.1}$, $PM_{2.5}$ and PM_{10}), though the correlations with Zn were not as good due to excess Zn, arising from tyre wear in the higher size fractions and lubricating oil in $PM_{0.1}$. Despite its complex source profiles, Zn concentrations were found to be quite consistent from day to day. The platinum-group elements Pt, Pd and Rh were not reported in $PM_{0.1}$ (Hays et al., 2011).

Pennanen et al. (2007) compared the water soluble metal fraction of $PM_{0.2}$ in six European cities. Levels of some trace elements such as Pb and Cd were found to be consistently low, but highly elevated levels of Ni and V were found in Helsinki and Barcelona, which is likely to reflect a shipping source. Elevated concentrations of several metals (Cr, Mn, Zn) were found in Duisburg, a city associated with metal industries (Pennanen et al., 2007).

The measurements of Lü et al. (2012) at an urban site in Shanghai showed that Fe, Cu and Ca were the most abundant metals in ultrafine particles, followed by V, Pb, Zn and As, with traces of Ti, Cr, Mn, Se and Rb. Of these element, only V and Cr showed ultrafine modes, although all appeared in the combined ultrafine samples. V, Cr and Ni also showed very high enrichment factors over crustal material in fine and ultrafine particles, but lower enrichments in coarse particles.

In an earlier paper, Lu et al. (2011) determined that metals in Shanghai aerosol could be divided into crustal/marine (Al, Ca, Fe, K, Mg and Na) and anthropogenic (As, Ba, Cd, Cr, Cu, Mn, Ni, Pb, Se, Sr and Zn) classes. Total metal mass was found to be highest in the coarse fraction for crustal elements and the fine fraction for anthropogenic elements. Iron showed the highest concentrations in the ultrafine, followed by copper and calcium. The authors also hypothesised that since calcium showed high mass concentrations and varied little between the size fractions, it was primarily crustal in source and participated in atmospheric reactions forming

Table 3
Outline of sampling techniques.

Instrument	Metric	Analysis	Size range (aerodynamic diameter)
MOUDI	Mass	Off-line	Model 100 (10-stage): 0.18, 0.32, 0.56, 1.0, 1.8, 3.2, 5.6, 10, 18 μm Model 110 (12-stage): also 0.056, 0.1 μm Models 115 and 116 include nano-stages: 0.01, 0.018, 0.032 μm
nanoMOUDI	Mass	Off-line	0.01, 0.018, 0.032, 0.056, 0.1, 0.18, 0.32, 0.56, 1.0, 1.8, 3.2, 5.6, 10 μm
ELPI	Mass	Off-line and on-line	0.007 μm Filter stage, 0.03, 0.06, 0.108, 0.17, 0.26, 0.4, 0.65, 1, 1.6, 2.5, 4.4, 6.8, 10
PCIS	Mass	Off-line	<0.25, 0.25–0.5, 0.5–1.0, 1.0–2.5 and 2.5 μm
BLPI	Mass	Off-line	0.035, 0.067, 0.093, 0.16, 0.32, 0.53, 0.94, 1.8, 3.5, 7.5 μm

secondary mineral particles in the fine and ultrafine ranges (Lu et al., 2011).

Ultrafine chemical composition data for metals at rural sites is not extensive, but some useful data have been published. Dodd et al. (1991) calculated modal diameters and enrichment factors of a number of metals relative to crustal aluminium in a study in rural Western Maryland. The aerosol fine structure in the sub-micron size fraction was found to be highly complex with most elements exhibiting more than one mode. Na, Ga, Ti, Al, La, Ce, and Fe all exhibited a narrow peak at 100 nm. The authors took such modes as representative of sources in high temperature combustion processes. Pakkanen et al. (2001) used low-pressure impactors to measure UFP composition at urban and rural sites in the Helsinki area and found that chemical composition was similar at both sites; in each case the most important metals in $\text{PM}_{0.1}$ were Ca, Na, Fe, K and Zn, concentrations varying between 0.7 and 5 ng/m^3 . The metals Ni, V, Pb and Cu were reported at concentrations in the 0.1–0.2 ng/m^3 range. Total ultrafine particle mass was reported to be 490 ng/m^3 at the urban site and 520 ng/m^3 at the rural site. The authors also stated that while the number of samples was too small to be certain of this, it appeared that concentrations were higher in summer at the rural site and no clear seasonal pattern could be seen at the urban site (Pakkanen et al., 2001). Daher et al. (2013) found that crustal metals (Al, Fe, K, Ca, Mg and Ti) were proportionally more important contributors to annually averaged $\text{PM}_{0.25}$ at a remote rural site than at heavily polluted urban sites (13–17% of total mass), while the remaining trace elements accounted for less than 1% of total mass. Furthermore, metals related to specific industrial sources such as Ni, and with shipping such as V and La, were present in much smaller concentrations than at urban sites. By comparison, concentrations of Fe and Al were much more similar between urban and rural sites (Daher et al., 2013; Saffari et al., 2013).

3.2. Temporal and spatial variability

A great deal of work has been published concerning this issue and has been summarised by other reviews (Morawska et al., 2008), but primarily refers to number distributions of total particles and not mass, as the longer collection times necessary for mass measurements tend to average out short-term variability. For mass data, the field is very limited at the present time.

Park et al. (2008c) reported that little variation in ultrafine particle concentration and composition was observed in Gwangju despite significant variation in PM_{10} (Park et al., 2008c). By comparison, Tolocka et al. (2005) reported significant differences in particle composition in Baltimore in the short term, influenced by local meteorology determining the impact of local sources on the receptor site, but not much seasonal or diurnal variation (Tolocka et al., 2005).

Saffari et al. (2013) have reported data showing that winter-time concentrations at a remote receptor site near Los Angeles were

lowest, but were higher at near-source sites. This was thought to reflect decreased mixing heights in cold weather. It was found that the highest summertime concentrations were recorded at the inland receptor sites, with metals peaking at urban sites in winter and downwind receptor sites in summer. Total $\text{PM}_{0.25}$ mass has been found to be rather uniform across the Los Angeles basin, but significant variations in the distribution of several toxic metals were observed, so that population exposures will be considerably different even across quite small spatial scales (Daher et al., 2013).

4. Instrumental techniques

4.1. Sampling instruments

Various forms of impactor-type instruments have been widely used in particulate matter sample collection, including Micro and nano-Micro Orifice Uniform Deposit Impactors (MOUDI and nanoMOUDI, manufactured by MSP corporation) and Low Pressure Impactors, their purpose being to collect size segregated particulate matter samples (see Table 3). The nanoMOUDI-ii 125 instrument has thirteen stages with nominal 50% cut-points of 10,000, 5600, 3200, 1800, 1000, 560, 320, 180, 100, 56, 32, 18 and 10 nm when operated at an inlet flow rate of 10.0 L/min. The instrument separates particles into a series of logarithmically equal size fractions based on aerodynamic diameter. Cascade impactor instruments such as the nanoMOUDI-ii can require long sampling times to collect sufficiently high masses of nanoparticulate material for accurate quantification of mass and chemical composition. Lu et al. (2011) found that it was necessary to combine the ultrafine filters for extraction and analysis, as one was persistently below limits of detection (Lu et al., 2011). The length of sampling periods have to be decided based on the limits of detection established for the analytical processes and the likely range of sampled concentrations, but in most published work using nanoMOUDIs, sampling times of several days are typical. One method of overcoming this problem is to set up the nanoMOUDI downstream of an aerosol concentrator; Ntziachristos et al. (2007) employed this method when sampling for 35 h (Ntziachristos et al., 2007) and Geller et al. (2002) also used a similar set-up in a study designed to investigate mass size distributions over relatively short (<24 h) timescales, which would preclude using such an instrument normally (Geller et al., 2002). The operation of such systems is described in more detail elsewhere (Kim et al., 2001; Geller et al., 2002), but in brief it enriches ultrafine particle concentrations by drawing in air at 220 L/min and growing particles to 2–3 μm by a saturation–condensation system and then passes the particles through diffusion dryers in order to return them to the original size distribution. The system is capable of up to 40-fold enrichment, although this depends on output flow rate; Geller et al. (2002) employed two parallel sampling lines, at an input rate of 110 L/min and output rate of 5 L/min, giving an enrichment factor of 22.

The MOUDI in its 10- and 12- stage forms has also been used for ultrafine particle collection (Cass et al., 2000), although it provides less resolution below 100 nm aerodynamic diameter than the nanoMOUDI. Currently available models have cut-points beginning at 180 nm in the standard 10-stage Model 100 but extra stages to give better size distribution data in the ultrafine size range are also available; the model 110 has 56 nm and a 100 nm cut-points below the 180 nm stage. The MOUDI samples at 30 L/min, allowing faster sample collection than the nanoMOUDI.

Other impactor designs available include the Personal Cascade Impactor Sampler (PCIS), a miniaturised 4 stage design operating at 9 L/min which is more easily portable than MOUDI/nanoMOUDI type instruments but offers no size segregation below 250 nm aerodynamic diameter (Misra et al., 2002b). Agreement with SMPS sizing data is reported to be good. Total mass concentration agrees well with MOUDI measurements even at below 250 nm, although the MOUDI underestimates slightly in this range compared to PCIS (PCIS:MOUDI = 1.09). This underestimate is thought to be caused by higher evaporative losses from the MOUDI after filter owing to the lower pressure, demonstrated by the PCIS:MOUDI ratio for nitrate in $PM_{0.25}$ being ~ 2.7 (Singh et al., 2003). The instrument has been successfully used in collecting quasi-ultrafine samples in ambient conditions (Saffari et al., 2013; Daher et al., 2013).

The development of an ultrafine separator to allow separation of particles below 150 nm in the High Volume Cascade Impactor was reported by Misra et al. (2002a). This instrument operates at 550 L/min and the authors reported that tests with monodisperse aerosol showed agreements with MOUDI data which were within 10% (Misra et al., 2002a). A further study by Sillanpää et al. (2003) compared three different configurations of the HVCI with a virtual impactor and a low-pressure impactor and concluded that the most effective set-up for aerosol configuration using this instrument was to use three HVCI stages with cutpoints of 2400, 900 and 200 nm with an Andersen PM_{10} inlet to remove material above 10 μm (Sillanpää et al., 2003). The HVCI has been used for ambient sampling of $PM_{0.2}$ in several European cities by Pennanen et al. (2007), along with the Berner low pressure impactor (BLPI). Good results were obtained although the water soluble metal samples extracted from the HVCI samples were found to be underestimated by comparison to BLPI (Pennanen et al., 2007). The method is clearly viable and the high sampling rate would be ideal for exposure studies, the major limitation being the lack of size segregation in the ultrafine size range. Another type of high volume sampler is the High Capacity Particle Size Classifier (HCPSC), an inertial impactor operating at 850 L/min and capable of collecting $PM_{0.15}$ (Chang et al., 2000). A field evaluation comparing the HCPSC to the MOUDI found that total mass, chloride, nitrate and sulphate all agreed within 10%, but also found that approximately 15% of fine mode particles are carried over to the ultrafine due to imperfect collection characteristics caused by the rectangular nozzle shape (Chang et al., 2001). The instrument has been used for ultrafine particle collection by Hetland et al. (2004), though not specifically for metals, (Hetland et al., 2004).

The Compact Multistage Cascade Impactor (CCI) developed at Harvard could also be used for sampling ultrafine/pseudo-ultrafine particulates. This instrument operates at 30 L/min and is designed to reduce particle bounce and re-entrainment loss by using inert polyurethane substrates. Particle losses per stage below 7000 nm have been reported to be below 10%. In comparison with the MOUDI, tests with artificially generated aerosol showed mass concentrations measuring persistently higher using CCI (MOUDI:CCI = 0.86). The size distributions were closer than MOUDI distributions to those calculated from real-time methods such as SMPS and APS; the comparative results were consistent with particle bounce in the MOUDI (Demokritou et al., 2004). The Harvard

CCI has been used with success to collect UPF in an exposure study measuring metals, ions and total PM mass associated with welding activities (Chang et al., 2013).

Berner-type low pressure impactors have also been widely used in many environmental research applications (Hughes et al., 1998; Pennanen et al., 2007; Pakkanen et al., 2001) and are capable, depending on the model (several instruments based on the same principle have been produced) of separations of particles down to aerodynamic diameters around 10 nm. The development of the commonest type was reported by Berner and Luerzer (1980) and the collection characteristics of the instrument have been well characterised (Wang and John, 1988; Hillamo and Kauppinen, 1991). Pakkanen et al. (2001) collected the following cut-points: 7500, 3500, 1800, 940, 530, 320, 160, 93, 67 and 35 nm equivalent aerodynamic diameter, based on the calculations of Hillamo and Kauppinen (1991), which differed slightly from the original 50% cut-points quoted by the manufacturer (Hauke).

The Electrical Low Pressure Impactor (ELPI) is now a widely used and well characterised system (Keskinen et al., 1992), capable of measuring particle mass distributions and particle number distributions depending on the mode of operation. Unlike MOUDI/nanoMOUDI type instruments, particle number data can be available in near-real-time, a significant advantage which allows better measurement of the time variation of the size distribution through the sampling period, rather than an integrated measurement over a long period. (Keskinen et al., 1992). The instrument consists of a corona charger mounted ahead of a cascade impactor. Particles are charged to a known level by the unipolar corona charger and passed into the impactor, where they are separated according to aerodynamic diameter and then can either be detected in real time by electrometers in each stage or collected for later analysis on filter substrates, as in MOUDI-type impactors. For real time number measurements, it has been shown through calibration tests with monodisperse aerosol that the distributions produced by the ELPI are in close agreement with Scanning Mobility Particle Sizer data (Marjamäki et al., 2000). Keskinen et al. (1992) also reported good agreement with differential mobility analyser data although the resolution was low compared to Differential Mobility Analysis when analysing aerosol of narrow size ranges. The technique has been successfully applied to size-segregated ultrafine particle studies incorporating trace metal analysis by Pakkanen et al. (2001) and Hays et al. (2011) in both background and near-highway settings. In both of these cases the instrument was used as a conventional impactor to collect filter samples for later offline analysis (Pakkanen et al., 2001; Hays et al., 2011).

Important considerations in the employment of impactors are sampling artefacts such as particle bounce and blow-off, which lead to larger particles being carried over into later stages producing less accurate size distributions. Some studies use coatings on the impaction surfaces to reduce this, but if chemical or gravimetric analysis is to be performed on the samples this may present problems. A recent study of interstage nanoparticle losses in the MOUDI concluded that particles below 40 nm aerodynamic diameter were significantly affected by interstage loss between the inlet and the lower stages (7–10). The authors also suggest that in the 13-stage MOUDI and nanoMOUDI instruments, interstage losses of nanoparticles would be even more serious. It was also observed that the nozzles in the 7th–10th stages clogged easily during sampling and must be cleaned regularly, otherwise an increase in the pressure drops will result and cause a decrease in the cut-points of these stages. However, since the plates are fragile it is not possible to use ultrasonic cleaning to remove deposited particles (Liu et al., 2013).

One method which has been used to mitigate these problems was reported by Cass et al. (2000), who used a cyclone impactor

upstream of the MOUDI to impose a cut of 1800 nm before the airstream entered the impactor. This reduced carryover of coarser material into the lower stages. Geller et al. (2002) achieved a similar effect by putting a 10 stage MOUDI with no afterfilter ahead of the nanoMOUDI, which prevented particles >180 nm D_a from entering the instrument. While effective, these techniques can only be employed if the study does not intend to measure coarser material.

During a study in Gwangju, Park et al. (2008c) used a Differential Mobility Analyser to size segregate particles, which were then collected onto TEM grids in a nano-aerosol sampler for offline TEM analysis (Park et al., 2008c).

4.1.1. Filter substrates

An important consideration in the employment of impactor-type instruments is the filter substrate on which the sample is deposited. There are numerous different types available which differ considerably in physical and chemical characteristics, including Al foils, quartz fibre filters, PTFE membrane filters and membrane filters made from cellulose nitrate or polycarbonate. Mechanical (to avoid biasing mass measurements) and chemical stability are paramount, especially given the small masses collected in ultrafine sampling. Similarly, low blank concentrations and low variability for the species of interest are crucial. Selection of filter type depends on the type of analytical procedure which will be applied and the subject under investigation. A number of publications are available which discuss this issue in depth (Chow, 1995; Wieprecht et al., 2004).

The studies referenced in Table 2 all utilised either PTFE or polycarbonate filters for collection of samples for metal analysis. Such substrates offer good particle retention and PTFE filters are non-reactive (Wieprecht et al., 2004). Although quartz filters are more resistant to artefact effects and moisture absorption (Wieprecht et al., 2004), they are also more brittle, which can lead to fibres being lost during handling introducing a negative mass bias (Chow, 1995). Ultrafine and nanoparticle sampling would be highly sensitive to such errors owing to the small sampled masses.

4.2. Off-line studies using electron microscopy

Bzdek et al. (2012) recently published a review of many of the most prominently used on-line and off-line techniques for the analysis of individual particles. They noted that it is crucially important that the sampled nanoparticles give an accurate representation of the particle classes and morphologies present in ambient air, but that off-line methods such as Transmission Electron Microscopy–X-ray–Energy Dispersive Spectroscopy (TEM–X–EDS) offer better characterisation of physical structure and chemical composition than on-line single particle techniques are currently able to do (Bzdek et al., 2012). Smith et al. (2012) observed that one weakness of TEM is a tendency to lose volatile material. This is not relevant to all metallic particles, but some elements do appear in volatile or semi-volatile material. Smith et al. (2012) also reported Na and K-bearing non-aggregated beam sensitive particles which they associated with inorganic salts. A further problem is that analysis by these techniques is laborious and time-consuming, so only relatively small numbers of particles from any given sample can be imaged and analysed, with a corresponding effect on the statistical validity of the results (Smith et al., 2012).

X-ray energy dispersive spectroscopy has been used to investigate the chemical composition at the individual particle level (Smith et al., 2012). Patel et al. (2012) did report, however, that zinc and calcium could only be detected by EDS in larger agglomerates, and not the primary particles ranging between 20 and 50 nm. They also established through comparison with results from selected area diffraction patterns that these elements were likely to be

present as compounds rather than in their elemental forms, and probably as amorphous structures (Patel et al., 2012).

Smith et al. (2012) identified 8 characteristic particle morphologies in fine/ultrafine urban particles during the REPARTEE study in London. Carbonaceous particles dominated the size ranges between 0.2 μm and 1.2 μm ; these particles were mainly aggregates of spherules composed either wholly of C or incorporating some O and sometimes Si. Amorphous aggregates similar to these were also observed containing metals. Ca, K and Fe were most common. Crystalline Fe oxide particles and Ca based particles, both amorphous and crystalline, were reported; the Ca particles showed strong peaks in Ca, O and C, along with Na, Al and Si. This is typical of mineral and soil based sources (Smith et al., 2012).

Adachi and Buseck (2010) also used TEM with EDS, reporting a range of trace metals in nanoparticles and determining that Fe was the commonest constituent (often associated with Cr, Mn and/or Ti), followed by Pb and Zn, which were frequently found together. They also examined co-existence in multimetallic particles in detail. However, their results also gave prominence to elements which are not generally emphasised in bulk studies. For instance, Hg was also detected in over 10% of nanoparticles, both in aggregates and adhered to host particles, and was quite beam sensitive. Hg has several known sources, of which fossil fuel combustion is most important globally, but local industrial sources may dominate at individual sampling locations (Adachi and Buseck, 2010).

Utsunomiya et al. (2004) examined trace metals in fine/ultrafine particulates from Detroit using TEM–X–EDS and gave particular prominence to Pb, found in the form of PbO included in carbonaceous soot, indicative of origin in fossil fuel combustion. Zn tended to occur in complex aggregates with other nanoparticles such as Fe, Si and Al oxides and phosphates. Some larger Fe–Zn particles (100–150 nm) were found to be $\text{Fe}_3\text{Zn}_{10}$, associated with metallurgical processes, and correlation analysis showed both metallurgical and fossil fuel sources (Utsunomiya et al., 2004).

Ultrafine material generated from the road-tyre interface has been reported to exhibit five major particle types, two of which are liquid (Dahl et al., 2006). The solid phase particles consist of single near-spherical particles and agglomerates of near-spherical particles, whose mobility diameters are between 10 and 100 nm. It is suggested that the spherical primary particles originate from carbon black used as a reinforcing filler though it is possible that small inclusions of ZnO or ZnS are responsible for the spherical morphology. The fractal structure of the agglomerates implies that they were detached under tensile stress rather than excessive heating, which would cause the chains to contract (Dahl et al., 2006).

Vehicle exhaust particles are typically the dominant source of ultrafine particulate matter, especially in urban areas and their characterisation is vital for assessing the effects of exposure. According to Tumolva et al. (2010), such particles are typically highly agglomerated with a high surface area to mass ratio, consisting of large numbers of small spherical carbon based primary particles. Diesel soot, which forms a large part of the total ultrafine particulate matter burden, has been the subject of a number of attempts to characterise physical as well as chemical characteristics more closely. A recent study (Lu et al., 2012) using TEM established that freshly emitted medium duty diesel engine particulate matter is generally composed of spherical or near spherical particles averaging 23.8 nm–28.5 nm diameter; however, the characteristics of the emitted particles were found to vary depending on engine speed and load, with low engine speeds and high loads generating larger primary particles. The study also discovered that higher engine speeds produce more disordered structures. (Lu et al., 2012). Tumolva et al. (2010) reported a mean primary particle diameter of

24 nm (SD 3.5 nm) for diesel soot produced in the laboratory, with a mean maximum length of 262 nm (SD 222 nm). This study also reported a relatively low fractal dimension of 1.69 for diesel exhaust particles, indicating a high level of branching in diesel particle agglomerate structures.

Jung et al. (2005) determined that CeO₂ additives in diesel engines contribute ceria to the particulate phase in two main morphological types. Firstly, fractal agglomerates of carbonaceous spherules of around 20–30 nm (the typical structure for diesel soot) with nanoparticulate cerium oxide (around 5–7 nm) adhered to the surface, and secondly, metallic aggregates formed from CeO₂ nanoparticles (5–7 nm) with some carbon. (Jung et al., 2005). The second particle class contains proportionally far more cerium than the first. They point out that the very high melting point of ceria (2200–2400 °C) means that a nanoparticulate ceria additive should remain unchanged through diesel combustion.

Some similar morphological characteristics for diesel engine derived metallic particles are also observed with the Fe fuel additives, depending on the level of doping. In a trial of ferrocene doping, Miller et al. (2007a) discovered that at low Fe concentrations (20 ppm doping level), exhaust particles exhibit typical diesel soot morphology, but above an Fe/C ratio of 0.013 the morphology switches to homogeneously nucleated metallic particles which form agglomerates across a wider size range. Miller et al. (2007a) reported two principal agglomeration modes, the first where 5–10 nm Fe nanoparticles attach to carbon agglomerates, and the second where larger iron agglomerates coagulate with carbon agglomerates. In this second case, the primary metallic particles can be so small they are not easily resolved by TEM, but can be observed through EDS spectra of large particles, implying it is present through vapour deposition onto carbon particles. Results suggest that particle size is dose-dependent, since iron primary particles are larger at higher doping levels (Miller et al., 2007a).

A more recent study of ferrocene fuel additives by Nash et al. (2013) assumes a formation process whereby Fe nucleates in the early phase of soot formation and then the Fe particles are incorporated in larger agglomerates in the exhaust. As well as the additive, substantial (>1000 ppm) concentrations of Ca and Zn were present in the lubricating oil along with smaller (<100 ppm) levels of Cu, Cr, Fe, Mg and Mn. A doping level of 25 ppm Fe was found to change the normal particle distribution (volume mean 80–90 nm) by introducing a second smaller mode. This effect, resulting in a reduction in volume and number concentrations in the accumulation mode and an increase in number and volume of nanoparticles, becomes more pronounced as the doping level increases. TEM analysis revealed that at 18 nm mean diameter, spherical and irregular morphologies are both present, attributed to Fe nuclei agglomerating to form clusters prior to soot formation and to Fe particles which coalesced and agglomerated after soot formation and oxidation. By comparison at 100 nm mean aerodynamic diameter, carbon agglomerates dominate, with Fe occlusions and surface deposits. Aerosol Time-of-Flight-Mass Spectrometry (ATOFMS) data demonstrated that almost all Fe was in the elemental form, with trace amounts of FeO but no Fe₂O₃. XRF showed that in undoped diesel exhaust Fe represents around 0.1% of the total particle mass, increasing to 1% at 25 ppm ferrocene. The distribution changes as iron content increases; at 25 ppm Fe, some 81% of the Fe content is in particles smaller than 56 nm, but at 200 ppm Fe, this falls to around 50% (Nash et al., 2013).

Buonanno et al. (2011) reported that ultrafine particles from an incinerator stack demonstrated a wide range of morphologies, including platelets and thin plates with indented and rounded edges. The stack emissions were found to contain high quantities of

metal oxides and silicates, with Fe, Fe–Cr, Zn, W–Fe–Cr and Ti oxides being prevalent (Buonanno et al., 2011).

4.3. On-line studies using aerosol mass spectrometry

Early ATOFMS systems required the particle to be >200 nm (optical diameter) to scatter the visible laser beam (Jayne et al., 2000). For particles below this limit, detection efficiency is strongly dependent on size and composition. Aerodynamic focusing lens systems have been developed to improve transmission efficiencies in the ultrafine, leading to the ultrafine-ATOFMS instrument, which has much improved particle sizing and detection efficiencies in this size range (Su et al., 2003). This technique has successfully been applied by Toner et al. (2006) to the source apportionment of ultrafine and accumulation mode particles arising from diesel and gasoline emissions. Zauscher et al. (2011) developed a water-based growth tube system which uses condensation to grow particles which would be too small for optical detection. This enables the detection and analysis of particles down to 38 nm (Zauscher et al., 2011).

The rapid single particle mass spectrometer (RSMS) has also been applied to single particle studies (Phares et al., 2003; Lake et al., 2003; Tolocka et al., 2004) with some success. Lake et al. (2003) were able to analyse ultrafine particles down to an aerodynamic diameter of 45 nm, determining that around 10% of sampled particles in an optimum range of 50–770 nm contained metals. Phares et al. (2003) reported detection of Al, Fe, K, Pb and V at the Houston supersite. A more detailed treatment of the technique was published by Reinard et al. (2007).

Park et al. (2009) reported the development of a Laser-Induced Breakdown Spectroscopy (LIBS) method which can be applied to investigate the chemical composition of particles down to around 60 nm, by employing an aerodynamic lens system to allow focusing of smaller particles. This method has been found to exhibit linear mass-peak area relationships for several metals, and to be able to detect internally mixed metal aerosols. Previously LIBS techniques had only been applied above lower limits of 200–400 nm and no reported results existed for particles below 100 nm (Park et al., 2009).

4.4. Source apportionment

A number of source apportionment techniques are widely used to examine airborne particulate matter data. The most widely used techniques fall under the category of receptor models such as Chemical Mass Balance (CMB), Principal Component Analysis (PCA) and Positive Matrix Factorisation (PMF), which use chemical and physical properties of PM to assign contributions to different sources. Applying these methods to mass concentration data of ultrafine and nanoparticles poses several challenges. Chemical mass balance can be a valuable method, providing that sources are already known and there is already detailed information concerning source profiles (Wang et al., 2012). This is a severe hindrance in applying this technique to ultrafine particle data where source profile information is sparse. If some sources are not known, or source profile information is limited, chemical mass balance is less useful; in such circumstances PCA and PMF are preferred (Srimuruganandam and Shiva Nagendra, 2012).

Principal Component Analysis has been successfully applied to PM_{0.25} metal composition data by Saffari et al. (2013), who used this technique to resolve data from 10 sites in the Los Angeles area into five separate components. The first component showed high loadings for mineral elements (Ca and Mg) and transition metals such as Fe, Co, Ti and Mn. This factor was attributed to road dust enriched by traffic-related emissions. PC2 was characterised by

high loadings (<0.7) for brake wear elements such as Ba, Cu and Sb. When PCA was applied separately to urban and receptor sites, Ba and Cu appeared in different factors. At urban sites, these elements were classed in the road dust factor, but formed a separate factor at receptor sites. The authors attributed this change to the dominance of vehicle emissions in urban areas making it more difficult to separate emission sources. Road dust was found to account for more of the total variance at urban sites (62%) compared to receptor sites (35%) (Saffari et al., 2013). Lin et al. (2005) also applied PCA to MOUDI and nanoMOUDI sample results from Pingtung, Taiwan. This study found four factors in nano/ultrafine particulates which corresponded to elements associated with diesel, gasoline, fuel oil and industrial emissions. They reported strong correlations between Ba, Pb and Zn in this size range, which supported a traffic source for these elements. The relative abundance for these elements in PM_{0.056–0.1} and PM_{0.056} was more similar to diesel emissions than to gasoline (Lin et al., 2005).

PMF is increasingly widely used for source apportionment. Unlike CMB, there is not a requirement for source profiles to be input into the model. However, in order to interpret the factors reported by the model as pollution sources, some knowledge of source profiles is still required (Wang et al., 2012). PMF can provide a robust solution provided that the sample:variable ratio is above 3:1. PMF is particularly suitable for analysing long time series, and observations need not be continuous for the method to work effectively. Assigning factors to sources is complex and to some extent subjective, as there are problems with the inconsistent use of species as source tracers (Reff et al., 2007). PMF results therefore have to be carefully interpreted. As of yet now, of PMF for nanoparticle source apportionment (especially mass-based) has been limited, owing to the difficulty of collecting enough samples to ensure the results are valid. Because of the long sampling times necessary, short term variations which would make factorisation easier tend to be averaged out, suppressing the impact of individual sources (Kumar et al., 2012).

5. Conclusion

While much progress has been made in understanding the sources contributing ultrafine particles to the atmosphere and characterising them in terms of particle number and size distributions, there is far less knowledge of the metal components of the ultrafine fraction. There is some knowledge of physical and chemical properties such as whether metals are free-floating or hosted on or within carbonaceous or mineral matrices, single particles or agglomerates. In some cases these properties have been associated with different source types. At this stage there are few studies reporting bulk ambient metal concentrations. Progress has been made in understanding how physical and chemical atmospheric processes affect ultrafine particles, and understanding how concentrations, composition and distribution vary in different environments. Progress has been made in establishing elements, compounds and particle types which are diagnostic of particular emission sources in larger size ranges, but their applicability to ultrafine particles is very limited.

Future research needs to consider the distribution of metals between size ranges, with a view to determining the chemical composition arising from different sources, especially as these may vary from the bulk, for example, the case of Al being less reliable as a crustal origin marker in ultrafine particles than coarse particles has been discussed.

The greatest weaknesses in characterising the metallic content of nanoparticles in the atmosphere derive directly from the very low concentrations present and the fact that these require very long sampling times for conventional analytical methods to give useful

data. Attempts at higher time resolution have to date had limited success although single particle techniques, and especially those based on mass spectrometric methods, offer the possibility of characterising both size and metal content of particles. However, current instruments have difficulties sampling particles right into the nanoparticle size range and low resolution mass spectrometry suffers from isobaric interference with ions derived from non-metallic species. Given the current rapid expansion in the use of nanomaterials in everyday consumer products, many of them metal-based, there is a pressing need for real-time measurements of specific nanoparticles. If nanoparticle measurement technology is to rise to the associated challenges, there is a need to develop instruments capable of the sensitivity and specificity needed to characterise nano-sized particles for a range of chemical constituents in real time. Much yet remains to be done to meet this objective.

Acknowledgement

The funding by the UK Natural Environment Research Council is gratefully acknowledged (grant reference number NERC NE/I008314/1).

References

- Adachi, K., Buseck, P.R., 2010. Hosted and free-floating metal-bearing atmospheric nanoparticles in Mexico City. *Environ. Sci. Technol.* 44, 2299–2304.
- Adachi, K., Tainosho, Y., 2004. Characterization of heavy metal particles embedded in tire dust. *Environ. Int.* 30, 1009–1017.
- Berner, A., Luerzer, C., 1980. Mass size distributions of traffic aerosols at Vienna. *J. Phys. Chem.* 84, 2079–2083.
- Bérubé, K.A., Jones, T.P., Williamson, B.J., Winters, C., Morgan, A.J., Richards, R.J., 1999. Physicochemical characterisation of diesel exhaust particles: factors for assessing biological activity. *Atmos. Environ.* 33, 1599–1614.
- Boogaard, H., Kos, G.P.A., Weijers, E.P., Janssen, N.A.H., Fischer, P.H., Van Der Zee, S.C., De Hartog, J.J., Hoek, G., 2011. Contrast in air pollution components between major streets and background locations: particulate matter mass, black carbon, elemental composition, nitrogen oxide and ultrafine particle number. *Atmos. Environ.* 45, 650–658.
- Buonanno, G., Ficco, G., Stabile, L., 2009. Size distribution and number concentration of particles at the stack of a municipal waste incinerator. *Waste Manag.* 29, 749–755.
- Buonanno, G., Stabile, L., Avino, P., Belluso, E., 2011. Chemical, dimensional and morphological ultrafine particle characterization from a waste-to-energy plant. *Waste Manag.* 31, 2253–2262.
- Bzdek, B.R., Ross Pennington, M., Johnston, M.V., 2012. Single particle chemical analysis of ambient ultrafine aerosol: a review. *J. Aerosol Sci.* 52, 109–120.
- Cass, G.R., Hughes, L.A., Bhave, P., Kleeman, M.J., Allen, J.O., Salmon, L.G., 2000. The chemical composition of atmospheric ultrafine particles. *Philos. Trans. R. Soc. Lond. Ser. Math. Phys. Eng. Sci.* 358, 2581–2592.
- Cassee, F.R., Van Balen, E.C., Singh, C., Green, D., Muijser, H., Weinstein, J., Dreher, K., 2011. Exposure, health and ecological effects review of engineered nanoscale cerium and cerium oxide associated with its use as a fuel additive. *Crit. Rev. Toxicol.* 41, 213–229.
- Cernuschi, S., Giugliano, M., Ozgen, S., Consonni, S., 2012. Number concentration and chemical composition of ultrafine and nanoparticles from WTE (waste to energy) plants. *Sci. Total Environ.* 420, 319–326.
- Chang, C., Demokritou, P., Shafer, M., Christiani, D., 2013. Physicochemical and toxicological characteristics of welding fume derived particles generated from real time welding processes. *Environ. Sci. Process. Impacts* 15, 214–224.
- Chang, M., Sioutas, C., Cassee, F.R., Fokkens, P.H.B., 2001. Field evaluation of a mobile high-capacity particle size classifier (HCPSC) for separate collection of coarse, fine and ultrafine particles. *J. Aerosol Sci.* 32, 139–156.
- Chang, M.C., Sioutas, C., Fokkens, P.H.B., Cassee, F.R., 2000. A mobile high-capacity particle size classifier (HCPSC) for separate collection of coarse, fine and ultrafine particles. *J. Aerosol Sci.* 31, 120–121.
- Chuang, H.-C., Fan, C.-W., Chen, K.-Y., Chang-Chien, G.-P., Chan, C.-C., 2012. Vasoactive alteration and inflammation induced by polycyclic aromatic hydrocarbons and trace metals of vehicle exhaust particles. *Toxicol. Lett.* 214, 131–136.
- Chow, J.C., 1995. Measurement methods to determine compliance with ambient air quality standards for suspended particles. *J. Air Waste Manag. Assoc.* 45, 320–382.
- Daher, N., Hasheminassab, S., Shafer, M.M., Schauer, J.J., Sioutas, C., 2013. Seasonal and spatial variability in chemical composition and mass closure of ambient ultrafine particles in the megacity of Los Angeles. *Environ. Sci. Process. Impacts* 15, 283–295.

- Dahl, A., Gharibi, A., Swietlicki, E., Gudmundsson, A., Bohgard, M., Ljungman, A., Blomqvist, G., Gustafsson, M., 2006. Traffic-generated emissions of ultrafine particles from pavement–tire interface. *Atmos. Environ.* 40, 1314–1323.
- Demokritou, P., Lee, S.J., Ferguson, S.T., Koutrakis, P., 2004. A compact multistage (cascade) impactor for the characterization of atmospheric aerosols. *J. Aerosol Sci.* 35, 281–299.
- Dodd, J.A., Ondov, J.M., Tuncel, G., Dzubay, T.G., Stevens, R.K., 1991. Multimodal size spectra of submicrometer particles bearing various elements in rural air. *Environ. Sci. Technol.* 25, 890–903.
- Garg, B.D., Cadle, S.H., Mulawa, P.A., Groblicki, P.J., Laroo, C., Parr, G.A., 2000. Brake wear particulate matter emissions. *Environ. Sci. Technol.* 34, 4463–4469.
- Geller, M.D., Kim, S., Misra, C., Sioutas, C., Olson, B.A., Marple, V.A., 2002. A methodology for measuring size-dependent chemical composition of ultrafine particles. *Aerosol Sci. Technol.* 36, 748–762.
- Gidney, J.T., Twigg, M.V., Kittelson, D.B., 2010. Effect of organometallic fuel additives on nanoparticle emissions from a gasoline passenger car. *Environ. Sci. Technol.* 44, 2562–2569.
- Gietl, J.K., Lawrence, R., Thorpe, A.J., Harrison, R.M., 2010. Identification of brake wear particles and derivation of a quantitative tracer for brake dust at a major road. *Atmos. Environ.* 44, 141–146.
- Gustafsson, M., Blomqvist, G., Gudmundsson, A., Dahl, A., Swietlicki, E., Bohgard, M., Lindbom, J., Ljungman, A., 2008. Properties and toxicological effects of particles from the interaction between tyres, road pavement and winter traction material. *Sci. Total Environ.* 393, 226–240.
- Hays, M.D., Cho, S.-H., Baldauf, R., Schauer, J.J., Shafer, M., 2011. Particle size distributions of metal and non-metal elements in an urban near-highway environment. *Atmos. Environ.* 45, 925–934.
- Heal, M.R., Kumar, P., Harrison, R.M., 2012. Particles, air quality, policy and health. *Chem. Soc. Rev.* 41, 6606–6630.
- Hetland, R.B., Cassee, F.R., Refsnes, M., Schwarze, P.E., Låg, M., Boere, A.J.F., Dybing, E., 2004. Release of inflammatory cytokines, cell toxicity and apoptosis in epithelial lung cells after exposure to ambient air particles of different size fractions. *Toxicol. Vitro* 18, 203–212.
- Hillamo, R.E., Kauppinen, E.I., 1991. On the performance of the bermer low pressure impactor. *Aerosol Sci. Technol.* 14, 33–47.
- Hughes, L.S., Cass, G.R., Gone, J., Ames, M., Olmez, I., 1998. Physical and chemical characterization of atmospheric ultrafine particles in the Los Angeles area. *Environ. Sci. Technol.* 32, 1153–1161.
- Jayne, J.T., Leard, D.C., Zhang, X., Davidovits, P., Smith, K.A., Kolb, C.E., Worsnop, D.R., 2000. Development of an aerosol mass spectrometer for size and composition analysis of submicron particles. *Aerosol Sci. Technol.* 33, 49–70.
- Jung, H., Kittelson, D.B., Zachariah, M.R., 2005. The influence of a cerium additive on ultrafine diesel particle emissions and kinetics of oxidation. *Combust. Flame* 142, 276–288.
- Kenneth, A.R., 1976. Silicon and aluminum in atmospheric aerosols: crust-air fractionation? *Atmos. Environ.* 10, 597–601.
- Keskinen, J., Pietarinen, K., Lehtimäki, M., 1992. Electrical low pressure impactor. *J. Aerosol Sci.* 23, 353–360.
- Kim, S., Jaques, P.A., Chang, M., Froines, J.R., Sioutas, C., 2001. Versatile aerosol concentration enrichment system (VACES) for simultaneous *in vivo* and *in vitro* evaluation of toxic effects of ultrafine, fine and coarse ambient particles Part I: development and laboratory characterization. *J. Aerosol Sci.* 32, 1281–1297.
- Kittelson, D., Watts, W., Johnson, J., Schauer, J., Lawson, D., 2006. On-road and laboratory evaluation of combustion aerosols—part 2: summary of spark ignition engine results. *J. Aerosol Sci.* 37, 931–949.
- Kleeman, M.J., Schauer, J.J., Cass, G.R., 1999. Size and composition distribution of fine particulate matter emitted from wood burning, meat charbroiling, and cigarettes. *Environ. Sci. Technol.* 33, 3516–3523.
- Kukutschová, J., Moravec, P., Tomášek, V., Matějka, V., Smolík, J., Schwarz, J., Seidlerová, J., Šafářová, K., Filip, P., 2011. On airborne nano/micro-sized wear particles released from low-metallic automotive brakes. *Environ. Pollut.* 159, 998–1006.
- Kumar, P., Pirjola, L., Ketzler, M., Harrison, R.M., 2012. Nanoparticle emissions from 11 non-vehicle exhaust sources – a review. *Atmos. Environ.* 67, 252–277.
- Kumar, P., Robins, A., Vardoulakis, S., Britter, R., 2010. A review of the characteristics of nanoparticles in the urban atmosphere and the prospects for developing regulatory controls. *Atmos. Environ.* 44, 5035–5052.
- Lahaye, J., Boehm, S., Chambrion, P., Ehrburger, P., 1996. Influence of cerium oxide on the formation and oxidation of soot. *Combust. Flame* 104, 199–207.
- Lake, D.A., Tolocka, M.P., Johnston, M.V., Wexler, A.S., 2003. Mass spectrometry of individual particles between 50 and 750 nm in diameter at the baltimore supersite. *Environ. Sci. Technol.* 37, 3268–3274.
- Lee, D., Miller, A., Kittelson, D., Zachariah, M.R., 2006. Characterization of metal-bearing diesel nanoparticles using single-particle mass spectrometry. *J. Aerosol Sci.* 37, 88–110.
- Lenin, M.A., Swaminathan, M.R., Kumaresan, G., 2013. Performance and emission characteristics of a DI diesel engine with a nanofuel additive. *Fuel* 109, 362–365.
- Liati, A., Dimopoulos Eggenschwiler, P., Müller Gubler, E., Schreiber, D., Aguirre, M., 2012. Investigation of diesel ash particulate matter: a scanning electron microscope and transmission electron microscope study. *Atmos. Environ.* 49, 391–402.
- Lin, C.-C., Chen, S.-J., Huang, K.-L., Hwang, W.-L., Chang-Chien, G.-P., Lin, W.-Y., 2005. Characteristics of metals in nano/ultrafine/fine/coarse particles collected beside a heavily trafficked road. *Environ. Sci. Technol.* 39, 8113–8122.
- Linak, W.P., Yoo, J.-I., Wasson, S.J., Zhu, W., Wendt, J.O.L., Huggins, F.E., Chen, Y., Shah, N., Huffman, G.P., Gilmour, M.I., 2007. Ultrafine ash aerosols from coal combustion: characterization and health effects. *Proc. Combust. Inst.* 31, 1929–1937.
- Liu, C.-N., Awasthi, A., Hung, Y.-H., Tsai, C.-J., 2013. Collection efficiency and inter-stage loss of nanoparticles in micro-orifice-based cascade impactors. *Atmos. Environ.* 69, 325–333.
- Lough, G.C., Schauer, J.J., Park, J.-S., Shafer, M.M., Deminter, J.T., Weinstein, J.P., 2004. Emissions of metals associated with motor vehicle roadways. *Environ. Sci. Technol.* 39, 826–836.
- Lu, T., Cheung, C.S., Huang, Z., 2012. Effects of engine operating conditions on the size and nanostructure of diesel particles. *J. Aerosol Sci.* 47, 27–38.
- Lu, S., Feng, M., Yao, Z., Jing, A., Yufang, Z., Wu, M., Sheng, G., Fu, J., Yonemochi, S., Zhang, J., 2011. Physicochemical characterization and cytotoxicity of ambient coarse, fine, and ultrafine particulate matters in Shanghai atmosphere. *Atmos. Environ.* 45, 736–744.
- Lü, S., Zhang, R., Yao, Z., Yi, F., Ren, J., Wu, M., Feng, M., Wang, Q., 2012. Size distribution of chemical elements and their source apportionment in ambient coarse, fine, and ultrafine particles in Shanghai urban summer atmosphere. *J. Environ. Sci.* 24, 882–890.
- Lyyrinen, J., Jokiniemi, J., Kauppinen, E.I., Joutsensaari, J., 1999. Aerosol characterization in medium-speed diesel engines operating with heavy fuel oils. *J. Aerosol Sci.* 30, 771–784.
- Marjamäki, M., Keskinen, J., Chen, D.R., Pui, D.Y.H., 2000. Performance evaluation of the electrical low-pressure impactor (ELPI). *J. Aerosol Sci.* 31, 249–261.
- Miller, A., Ahlstrand, G., Kittelson, D., Zachariah, M., 2007a. The fate of metal (Fe) during diesel combustion: morphology, chemistry, and formation pathways of nanoparticles. *Combust. Flame* 149, 129–143.
- Miller, A.L., Stipe, C.B., Habjan, M.C., Ahlstrand, G.G., 2007b. Role of lubrication oil in particulate emissions from a hydrogen-powered internal combustion engine. *Environ. Sci. Technol.* 41, 6828–6835.
- Misra, C., Kim, S., Shen, S., Sioutas, C., 2002a. A high flow rate, very low pressure drop impactor for inertial separation of ultrafine from accumulation mode particles. *J. Aerosol Sci.* 33, 735–752.
- Misra, C., Singh, M., Shen, S., Sioutas, C., Hall, P.M., 2002b. Development and evaluation of a personal cascade impactor sampler (PCIS). *J. Aerosol Sci.* 33, 1027–1047.
- Moldanová, J., Fridell, E., Popovicheva, O., Demirdjian, B., Tishkova, V., Faccinotto, A., Fosca, C., 2009. Characterisation of particulate matter and gaseous emissions from a large ship diesel engine. *Atmos. Environ.* 43, 2632–2641.
- Morawska, L., Wang, H., Ristovski, Z., Jayaratne, E., Johnson, G., Cheung, H.C., Ling, X., He, C., 2009. Jem spotlight: environmental monitoring of airborne nanoparticles. *J. Environ. Monit.* 11, 1758–1773.
- Morawska, L., Ristovski, Z., Jayaratne, E., Keogh, D.U., Ling, X., 2008. Ambient nano and ultrafine particles from motor vehicle emissions: characteristics, ambient processing and implications on human exposure. *Atmos. Environ.* 42, 8113–8138.
- Nash, D.G., Swanson, N.B., Preston, W.T., Yelverton, T.L.B., Roberts, W.L., Wendt, J.O.L., Linak, W.P., 2013. Environmental implications of iron fuel borne catalysts and their effects on diesel particulate formation and composition. *J. Aerosol Sci.* 58, 50–61.
- Nixon, J.D., Wright, D.G., Dey, P.K., Ghosh, S.K., Davies, P.A., 2013. A comparative assessment of waste incinerators in the UK. *Waste Manag.* 33, 2234–2244.
- Ntziachristos, L., Ning, Z., Geller, M.D., Sheesley, R.J., Schauer, J.J., Sioutas, C., 2007. Fine, ultrafine and nanoparticle trace element compositions near a major freeway with a high heavy-duty diesel fraction. *Atmos. Environ.* 41, 5684–5696.
- Pakkanen, T.A., Kerminen, V.-M., Korhonen, C.H., Hillamo, R.E., Aarnio, P., Koskentalo, T., Maenhaut, W., 2001. Urban and rural ultrafine (PM_{0.1}) particles in the helsinki area. *Atmos. Environ.* 35, 4593–4607.
- Park, K., Cho, G., Kwak, J.-H., 2009. Development of an aerosol focusing-laser induced breakdown spectroscopy (aerosol focusing-libs) for determination of fine and ultrafine metal aerosols. *Aerosol Sci. Technol.* 43, 375–386.
- Park, B., Donaldson, K., Duffin, R., Tran, L., Kelly, F., Mudway, I., Morin, J.-P., Guest, R., Jenkinson, P., Samaras, Z., Giannouli, M., Kouridis, H., Martin, P., 2008a. Hazard and risk assessment of a nanoparticulate cerium oxide-based diesel fuel additive—A case study. *Inhal. Toxicol.* 20, 547–566.
- Park, K., Heo, Y., Putra, H., 2008b. Ultrafine metal concentration in atmospheric aerosols in urban Gwangju, Korea. *Aerosol Air Qual. Res.* 8, 411–422.
- Park, K., Park, J.Y., Kwak, J.-H., Cho, G.N., Kim, J.-S., 2008c. Seasonal and diurnal variations of ultrafine particle concentration in urban Gwangju, Korea: observation of ultrafine particle events. *Atmos. Environ.* 42, 788–799.
- Patel, M., Azanza Ricardo, C.L., Scardi, P., Aswath, P.B., 2012. Morphology, structure and chemistry of extracted diesel soot—part I: transmission electron microscopy, Raman spectroscopy, X-ray photoelectron spectroscopy and synchrotron X-ray diffraction study. *Tribol. Int.* 52, 29–39.
- Pennanen, A.S., Sillanpää, M., Hillamo, R., Quass, U., John, A.C., Branis, M., Hünová, I., Meliefste, K., Janssen, N.A.H., Koskentalo, T., Castaño-Vinyals, G., Bouso, L., Chalbot, M.C., Kavouras, I.G., Salonen, R.O., 2007. Performance of a high-volume cascade impactor in six European urban environments: mass measurement and chemical characterization of size-segregated particulate samples. *Sci. Total Environ.* 374, 297–310.
- Phares, D.J., Rhoads, K.P., Johnston, M.V., Wexler, A.S., 2003. Size-resolved ultrafine particle composition analysis 2. *Houston. J. Geophys. Res. Atmos.* 108, 8420.

- Ragazzi, M., Tirlor, W., Angelucci, G., Zardi, D., Rada, E.C., 2013. Management of atmospheric pollutants from waste incineration processes: the case of Bozen. *Waste Manag. Res.* 31, 235–240.
- Reff, A., Eberly, S.I., Bhave, P.V., 2007. Receptor modeling of ambient particulate matter data using positive matrix factorization: review of existing methods. *J. Air Waste Manag. Assoc.* 57, 146–154.
- Reinard, M.S., Adou, K., Martini, J.M., Johnston, M.V., 2007. Source characterization and identification by real-time single particle mass spectrometry. *Atmos. Environ.* 41, 9397–9409.
- Saffari, A., Daher, N., Shafer, M.M., Schauer, J.J., Sioutas, C., 2013. Seasonal and spatial variation of trace elements and metals in quasi-ultrafine (PM_{0.25}) particles in the Los Angeles Metropolitan area and characterization of their sources. *Environ. Pollut.* 181, 14–23.
- Sillanpää, M., Hillamo, R., Mäkelä, T., Pennanen, A.S., Salonen, R.O., 2003. Field and laboratory tests of a high volume cascade impactor. *J. Aerosol Sci.* 34, 485–500.
- Singh, M., Misra, C., Sioutas, C., 2003. Field evaluation of a personal cascade impactor sampler (PCIS). *Atmos. Environ.* 37, 4781–4793.
- Smith, S., Ward, M., Lin, R., Brydson, R., Dall'osto, M., Harrison, R.M., 2012. Comparative study of single particle characterisation by transmission electron microscopy and time-of-flight aerosol mass spectrometry in the London atmosphere. *Atmos. Environ.* 62, 400–407.
- Song, J., Wang, J., Boehman, A.L., 2006. The role of fuel-borne catalyst in diesel particulate oxidation behavior. *Combust. Flame* 146, 73–84.
- Srimuruganandam, B., Shiva Nagendra, S.M., 2012. Application of positive matrix factorization in characterization of PN10 and PM2.5 emission sources at urban roadside. *Chemosphere* 88, 120–130.
- Su, Y., Sipin, M.F., Furutani, H., Prather, K.A., 2003. Development and characterization of an aerosol time-of-flight mass spectrometer with increased detection efficiency. *Anal. Chem.* 76, 712–719.
- Thorpe, A., Harrison, R.M., 2008. Sources and properties of non-exhaust particulate matter from road traffic: a review. *Sci. Total Environ.* 400, 270–282.
- Tissari, J., Lyyränen, J., Hytönen, K., Sippula, O., Tapper, U., Frey, A., Saarnio, K., Pennanen, A. S., Hillamo, R., Salonen, R.O., Hirvonen, M.R., Jokiniemi, J., 2008. Fine particle and gaseous emissions from normal and smouldering wood combustion in a conventional masonry heater.
- Tolocka, M.P., Lake, D.A., Johnston, M.V., Wexler, A.S., 2004. Number concentrations of fine and ultrafine particles containing metals. *Atmos. Environ.* 38, 3263–3273.
- Tolocka, M.P., Lake, D.A., Johnston, M.V., Wexler, A.S., 2005. Size-resolved fine and ultrafine particle composition in Baltimore, Maryland. *J. Geophys. Res. Atmos.* 110, D07S04.
- Toner, S.M., Sodeman, D.A., Prather, K.A., 2006. Single particle characterisation of ultrafine and accumulation mode particles from heavy duty diesel vehicles using aerosol time-of-flight mass spectrometry. *Environ. Sci. Technol.* 40, 3912–3921.
- Tumolva, L., Park, J.-Y., Kim, J.-S., Miller, A.L., Chow, J.C., Watson, J.G., Park, K., 2010. Morphological and elemental classification of freshly emitted soot particles and atmospheric ultrafine particles using the TEM/EDS. *Aerosol Sci. Technol.* 44, 202–215.
- Utsunomiya, S., Jensen, K.A., Keeler, G.J., Ewing, R.C., 2004. Direct Identification of trace metals in Fine and ultrafine particles in the Detroit urban atmosphere. *Environ. Sci. Technol.* 38, 2289–2297.
- Wang, Y., Hopke, P.K., Xia, X., Chalupa, D.C., Utell, M.J., 2012. Source apportionment of airborne particulate matter using inorganic and organic species as tracers. *Atmos. Environ.* 55, 525–532.
- Wang, H.-C., John, W., 1988. Characteristics of the berner impactor for sampling inorganic ions. *Aerosol Sci. Technol.* 8, 157–172.
- Wieprecht, W., Acker, K., Müller, K., Spindler, G., Brüggemann, E., Maenhaut, W., Chi, X., Hitzenberger, R., Bauer, H., Brink, H.T., 2004. INTERCOMP2000: ionic constitution and comparison of filter and impactor. *Atmos. Environ.* 38, 6477–6486.
- Zauscher, M.D., Moore, M.J.K., Lewis, G.S., Hering, S.V., Prather, K.A., 2011. Approach for measuring the chemistry of individual particles in the size range critical for cloud formation. *Anal. Chem.* 83, 2271–2278.